One-Dimensional Instability in $BaVS_3$

Sebastien Fagot,[1] Pascale Foury-Leylekian,[1] Sylvain Ravy,[1] Jean-Paul Pouget,[1] and Helmuth Berger[2]
[1]*Laboratoire de Physique des Solides (CNRS-UMR 8502), Université Paris-Sud, Bâtiment 510, 91405 Orsay CEDEX, France*
[2]*Institute of Complex Matter, EPFL, CH-1015, Lausanne, Switzerland*
(Received 8 October 2002; published 13 May 2003)

The $3d^1$ system $BaVS_3$ undergoes a series of remarkable electronic phase transitions. We show that the metal-insulator transition at $T_{MI} = 70$ K is associated with a structural transition announced by a huge regime of one-dimensional (1D) lattice fluctuations, detected up to 170 K. These 1D fluctuations correspond to a $2k_F = c^*/2$ charge-density wave (CDW) instability of the d_{z^2} electron gas. We discuss the formation below T_{MI} of an unconventional CDW state involving the condensation of the other V^{4+} $3d^1$ electrons of the quasidegenerate $e(t_{2g})$ orbitals. This study stresses the role of the orbital degrees of freedom in the physics of $BaVS_3$ and reveals the inadequacy of current first principle band calculations to describe its electronic ground state.

DOI: 10.1103/PhysRevLett.90.196401 PACS numbers: 71.30.+h, 61.10.–i, 71.45.Lr

Low dimensional metals are extensively studied because they exhibit a large variety of quantum phenomena (superconductivity, quantum Hall effect, charge and spin density waves, orbital ordering), due to the balance between electron-electron correlations and the electron-phonon coupling [1]. Of particular interest is the charge-spin decoupling (Luttinger-liquid behavior) occurring when strong electron-electron correlations are present and leading to a metal-insulator transition associated to Mott-Hubbard localization and charge ordering. Well documented realizations of such features can be found among the transition metal oxides and organic conductors [2]. However, not so much is known from the transition metal sulfides. In this context, the metallic system $BaVS_3$ is of particular interest because photoemission studies suggest a Luttinger-liquid behavior [3] while transport and magnetic measurements show the occurrence of low temperature (LT) phase transitions in which charge and spin degrees of freedom are decoupled. In this paper, we present an x-ray study of the LT phase transitions of $BaVS_3$.

The room temperature (RT) structure of $BaVS_3$ [4] consists of a hexagonal packing of chains of face sharing VS_6 octahedra directed along the c axis. Its space group is $P6_3/mmc$, with RT unit cell parameters: $a_H = 0.672$ nm and $c_H = 0.562$ nm. The intrachain V-V distances (0.28 nm) being much smaller than the interchain distances (0.672 nm), $BaVS_3$ appears to be structurally a 1D compound although its resistivity anisotropy ratio is only 4 [5]. This sulfide undergoes three second-order LT phase transitions at $T_S = 240$ K, $T_{MI} = 70$ K, and $T_X = 30$ K. At T_S, a zigzag displacement of the V atoms inside the chains of octahedra induces a structural transition to an orthorhombic phase of unit cell parameters: $a_O = 0.675$ nm, $b_O = 1.148$ nm $< \sqrt{3}a_O$, and $c_O = 0.56$ nm and $Cmc2_1$ space group [6], which has been recently questioned in Ref. [7]. There is no significant change of the conducting properties at T_S.

At T_{MI}, $BaVS_3$ undergoes a metal to insulator transition. Above T_{MI}, $BaVS_3$ exhibits a paramagnetic conducting phase with a nearly temperature independent resistivity [8,9], showing a weak minimum at $\sim$140 K [5,10]. At T_{MI}, a rapid increase of the electrical resistivity (accompanied by an inflexion point around 60 K) [9,10], a change of slope in the thermal variation of the lattice parameters [11], and a specific heat anomaly [12] are observed. At LT, the gap of charge is estimated in the range 350 K [9]–600 K [5,11]. The magnetic susceptibility exhibits a sharp maximum at T_{MI} suggesting the occurrence of a magnetic transition. However, no long range magnetic order has been detected below T_{MI}, but recent neutron and NMR measurements rather suggest the formation of a spin gap estimated to be between 120 K [13] and 250 K [14]. The magnetic susceptibility remains finite at T_X, showing that the spin degrees of freedom are not completely frozen. Indeed, neutron scattering experiments [15] have provided evidence of an incommensurate magnetic modulation below T_X, although a recent NMR/NQR study [14] has shown that the ground state is nonmagnetic with a possible orbital ordering.

The electronic structure of $BaVS_3$ has been calculated using linear augmented plane waves and first principle methods [16,17]. The result shows that three bands cut the Fermi level: a 1D one associated to the d_{z^2} orbitals, with a 1 eV dispersion width in the chain direction, and two very narrow isotropic ones associated to the degenerate $e(t_{2g})$ orbitals split by the trigonal crystal field. The 1D band is found to be nearly filled by the two V^{4+} d^1 electrons of the unit cell, with a Fermi wave vector $k_F \sim 0.47c^*$ [17].

After the completion of this experimental work, an independent structural study [7] showed, in agreement with our results, that a structural modulation is stabilized at T_{MI} at the $(1\ 0\ 1/2)_O$ reduced wave vector. Here we prove that this transition is driven by huge pretransitional structural 1D fluctuations, showing that its driving force is essentially 1D in nature.

X-ray diffuse scattering investigations have been performed using the $\lambda_{Mo} = 0.0711$ nm radiation issued from either a classical tube or a rotating anode equipped with a doubly bent graphite monochromator. The investigation has been first performed with the so-called fixed film-fixed crystal method in order to detect the structural modulation and the weak x-ray diffuse scattering. Then accurate measurements of the satellite reflection intensity and of the diffuse scattering above the transition were performed using a three-circle diffractometer. The setup is equipped with closed cycle helium cryostat operating from 300 K down to 15 K. Three single crystals (2 mm $\times$ 0.2 mm) were studied.

Figure 1(a) presents an x-ray pattern of $BaVS_3$ taken at 80 K. Diffuse lines perpendicular to the c axis and located halfway between layers of main Bragg reflections are clearly visible. These lines correspond to the intersection of the Ewald sphere with diffuse sheets perpendicular to the c axis in the reciprocal space [18]. In direct space, this corresponds to pretransitional structural fluctuations with the critical wave vector $q_c = 0.5c^*$, correlated in the chain direction but decoupled between neighboring chains. Upon cooling below $T_C = 70 \pm 2$ K, the diffuse lines condense into satellite reflections [see Fig. 1(b)]. Within experimental errors T_C corresponds to T_{MI}. These satellite reflections are due to the stabilization of a commensurate structural modulation at the metal-insulator transition. The reduced wave vector of the satellite reflections in the orthorhombic cell is either $(1\ 0\ 1/2)_O$ or $(1/2\ 1/2\ 1/2)_O$ with an indetermination due to the presence of symmetry equivalent crystallographic domains induced at T_S by the hexagonal to orthorhombic transition. However, the $q_{MI} = (1\ 0\ 1/2)_O$ wave vector is in agreement with the one found in the single domain crystal study of Ref. [7] and will be used in the following. Finally, note that upon cooling down to 15 K (i.e., below $T_X = 30$ K) our photographic investigation did not reveal additional satellite reflections.

An accurate investigation of the thermal dependence of the intensity of several q_{MI} satellite reflections has been performed. At 20 K, the intensity of the satellite reflections is about 10^{-2} that of the main Bragg reflections. Figure 2 presents the thermal variation of the $Q = (\bar{2}\ 4\ \bar{3}) + q_{MI} = (\bar{1}\ 4\ \bar{2}.5)$ satellite reflection peak intensity $I(T)$. Upon cooling below $T_C = 70 \pm 2$ K, the intensity increases with a quasilinear slope, a feature expected for a second order transition in the mean field approximation. However, two slope anomalies can be detected at $\sim$65 and $\sim$58 K. No anomaly has been detected at T_X. In order to check the presence of $2q_{MI}$ harmonics, we have accurately measured the thermal dependence of the intensity of several Bragg reflections. The inset of Fig. 2 shows the thermal dependence of the integrated intensity for the $Q = (\bar{1}\ 5\ \bar{1}) + 2q_{MI} = (1\ 5\ 0)$ Bragg reflection. The curve $I(T)$ exhibits an anomaly at T_C . At 20 K, the relative intensity increase is 7%, which is about 10 times larger than the average satellite intensity. This suggests the existence of two order parameters at q_{MI} and $2q_{MI}$.

In the pretransitional fluctuation regime above T_C, we have measured the profile of the diffuse scattering along the three main orthorhombic directions $a_O = a_H$, $b_O = a_H + 2b_H$, and $c_O = c_H$ until 170 K. The data analysis was performed by using Lorentzian profiles convoluted with the experimental resolution. The half width at half maximum (HWHM) Δq obtained by this procedure gives the inverse correlation length ξ^{-1} of the fluctuations. Figure 3 presents the thermal variations of ξ^{-1} deduced from the measurements close to the $(\bar{1}\ 4\ \bar{2}.5)$ reciprocal position. The correlation lengths along the three crystallographic directions diverge at T_C, as expected for a second order phase transition. The correlation lengths are nearly isotropic in the (a_O, b_O) plane. They rapidly

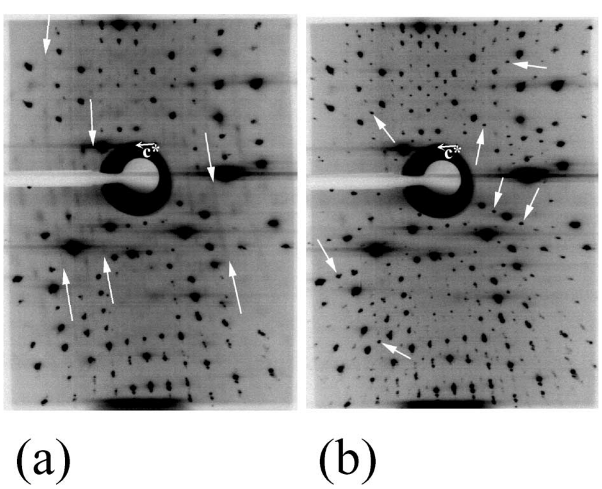

FIG. 1. X-ray patterns taken from $BaVS_3$ at 80 K (a) and 25 K (b), $\mathbf{c}^*$ is close to the horizontal direction. In (a) the arrows point towards the diffuse lines, and in (b) they point towards the q_{MI} satellite reflections.

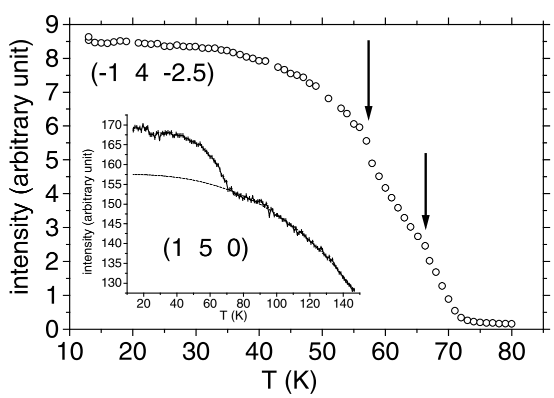

FIG. 2. Thermal dependence of the $(\bar{1}\ 4\ \bar{2}.5)$ peak intensity $I(T)$. The arrows indicate the anomalies at 65 and 58 K. In the inset, thermal dependence of the integrated intensity of the (1 5 0) Bragg reflection.

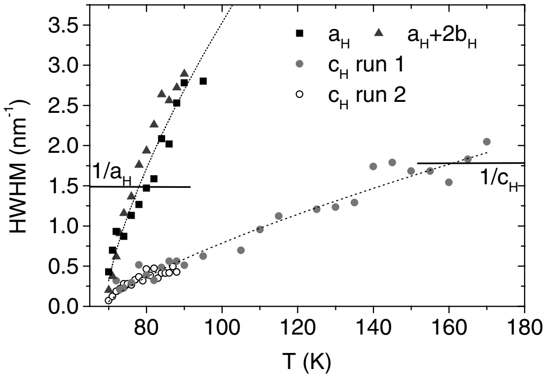

FIG. 3. Thermal dependence of the deconvoluted HWHM of the ($\bar{1}$ 4 $\bar{2}$.5) peak along the a_H, $a_H + 2b_H$, and c_H directions. The inverse of the a and c parameters is indicated.

decrease and reach a value smaller than the V-V interchain distance above ~80 K. On the other hand, the correlation length along the c_H axis decreases smoothly, reaching a value of 0.6 nm (corresponding to the c_H parameter) above 160 K. The 1D fluctuations are thus observed between 80 and 170 K, in a temperature range larger than T_C itself, and the crossover towards the regime of 3D fluctuations occurs at 80 K, about 10 K above T_C.

From these results, it appears that 1D fluctuations drive the metal-insulator transition of $BaVS_3$. Interestingly enough, the intrachain correlation length begins to grow sizably below about 150 K, which corresponds to the temperature at which the resistivity exhibits a broad minimum [5,10]. Below this temperature, the slight decrease of conductivity can thus simply be explained by the formation of a pseudogap in the charge degrees of freedom due to the coupling with the structural fluctuations [19]. Because of the presence of 1D fluctuations, the 3D ordering occurs at a critical temperature T_{MI} much lower than the mean field temperature of the chain T_{MF}. If one assumes that the gap of charge Δ_c is related to T_{MF} by the BCS relationship $\Delta_c = 1.76kT_{MF}$, and if T_{MF} is taken as the temperature (~170 K) at which the structural fluctuations begin to be detected, one gets $\Delta_c \sim 300$ K, a value in agreement with the results of Ref. [9].

The presence of a metal-insulator transition with 1D structural fluctuations suggests the occurrence of a Peierls transition, and, via the electron-phonon coupling, the formation of a charge-density wave (CDW) at the $2k_F$ critical wave vector of the 1D electron gas [19]. However, several features show that the physics of $BaVS_3$ is not so straightforward. First, the experimental value of q_{MI}, whose component along the chain is $2k_F = 0.5c^*$, shows that only one electron participates to the CDW among the two d^1 electrons of the unit cell. Second, the physical properties of $BaVS_3$ are not those of a standard CDW system [19]: The magnetic susceptibility exhibits a Curie-Weiss dependence instead of the expected Pauli behavior of a 1D metal of delocalized electrons, and its thermal dependence is not clearly affected by the growth of the pseudogap. All these features can be rationalized if one assumes that conduction electrons of different type (i.e., occupying different t_{2g} orbitals) are present in $BaVS_3$: delocalized d_{z^2} electrons responsible for the metallic character and the CDW instability, and localized $e(t_{2g})$ electrons responsible for the Curie-Weiss behavior [8]. In this context, although the formal valence of the V is V^{4+} in $BaVS_3$, the effective moment deduced from the Curie-Weiss behavior of the magnetic susceptibility ranges from $1.1\mu_B$ [3] to $1.33\mu_B$ [11], values consistent with one $S = 1/2$ spin every other V^{4+} [20]. This indicates that (i) one localized electron must occupy one every other V^{4+} site [and be shared between the two quasidegenerate $e(t_{2g})$ orbitals] and, consequently, that (ii) the d_{z^2} band is half filled. The later conclusion is in perfect agreement with our $2k_F$ determination. Unfortunately, this interpretation is not supported by *ab initio* band calculations [16,17], which give a $2k_F$ value 2 times larger (~$0.94c^*$). This discrepancy could be due to the presence of disordered and strongly interacting electrons in the $e(t_{2g})$ orbitals, making inaccurate the determination of the relative filling between the t_{2g} levels.

Concerning the $3d_{z^2}$ CDW transverse ordering, it corresponds to an out of phase ordering in the diagonal $a_H + b_H$ and b_H directions (see Fig. 4), as deduced from the condition $h + k = 2n + 1$ satisfied by the satellite reflection indices. This phasing between the nearest chains is likely to be due to the Coulomb repulsion between CDWs.

Our data show that the $3d_{z^2}$ electrons form a CDW below T_{MI}. However, although the condensation of the d_{z^2} electrons in a CDW leads to the suppression of the Pauli susceptibility, this cannot quantitatively explain the strong decrease of the susceptibility at T_{MI}. This clearly indicates that the $e(t_{2g})$ electrons are involved in the transition and order below T_{MI}. This hypothesis is reinforced by the presence of a strong $2q_{MI}$ modulation,

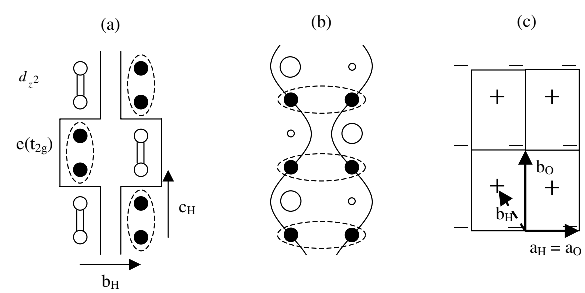

FIG. 4. Schematic representation of the hybrid CDW in the chain direction and the transverse direction. (a) Scenario involving the V^{4+}-V^{4+} bipolarons and a square shaped CDW. (b) Scenario involving the orbital ordering (circle size is a function of the electronic density). The possible $e(t_{2g})$ spin pairing is indicated by dashed lines. (c) CDW phasing in the (a_O, b_O) plane.

which indicates a deviation from a conventional CDW structure. Two scenarios can be suggested. One is that a hybrid CDW is constituted of $3d_{z^2}$ electrons forming V^{4+}-V^{4+} pairs (or bipolarons) separated by two $e(t_{2g})$ electrons achieving a $2c$ periodicity, but with a strong $2q_{\mathrm{MI}}$ harmonic [Fig. 4(a)]. In this case (i) the $e(t_{2g})$ orbital degrees of freedom would be preserved and could be involved at lower temperature and (ii) a spin pairing would be achieved along the chains. The second possibility is a $4k_F = c^*$ charge and orbital ordering associated to the CDW. The stabilization of a Jahn-Teller distortion usually associated with such orbital ordering could explain the strong amplitude of the observed $2q_{\mathrm{MI}}$ structural modulation. In this scenario, the spin pairing would take place transversally [see Fig. 4(b)].

These two ground states differ by their symmetry and should be distinguished by low temperature structural refinements. In both cases, the presence of two coupled order parameters (CDW and charge or orbital ordering) developing below T_{MI} could account for the thermal anomalies we have observed in $I(T)$. In this respect, it is noteworthy that an unusual thermal dependence in the rate of increase of the electrical resistivity is observed around 60 K [9], the temperature at which slope anomalies occur in $I(T)$ (Fig. 2). Concerning the magnetic properties, a spin pairing mechanism of the $e(t_{2g})$ electrons (either longitudinal or transverse) can be proposed in both cases. However, the report of an incommensurate transverse magnetic modulation below T_X [15] is not easy to integrate in the previous scenarios, and reinforces the need for theoretical and experimental efforts to understand the complex interplay between spin, charge, and orbital degrees of freedom in $BaVS_3$.

In conclusion, we have shown that the metal-insulator transition of $BaVS_3$ is driven by a 1D instability of the electron gas. This emphasizes the role of the 1D physics in this compound, which may be at the origin of the Luttinger-liquid behavior observed by photoemission spectroscopy [3]. The presence of a strong $4k_F$ component associated to the $3d_{z^2}$ CDW is interpreted as an ordering of the $e(t_{2g})$ electrons. In this respect, the occurrence of successive second order phase transitions observed in $BaVS_3$ has to be contrasted with the first order metal-insulator transition exhibited by VO_2, which, by removing the $e(t_{2g})$ orbital degrees of freedom, stabilizes a $3d_{z^2}$ V^{4+}-V^{4+} paired ground state [2]. Finally, this work stresses the limitations of current first principle methods to calculate the electronic structure of $BaVS_3$, despite the recent success obtained in describing low-dimensional electronic systems [21].

The sample preparation in Lausanne was supported by the NCCR research pool "MaNEP of the Swiss NSF. The LEPES-CNRS samples were synthesized by J. J. Since. E. Canadell and M. H. Whangbo are thanked for very useful discussions.

[1] S. Sachdev, Electronic cooperation, Science **288**, 475 (2000).

[2] M. Imada, A. Fujimori, and Y. Tokura, Rev. Mod. Phys. **70**, 1039 (1998).

[3] M. Nakamura, A. Sekiyama, H. Namatame, A. Fujimori, H. Yoshihara, T. Ohtani, A. Misu, and M. Takano, Phys. Rev. B **49**, 16 191 (1994).

[4] R. Gardner, M. Vlasse, and A. Wold, Acta Crystallogr. Sect. B **25**, 781 (1969).

[5] G. Mihaly, I. Kezsmarki, F. Zamborszky, M. Miljak, K. Penc, P. Fazekas, H. Berger, and L. Forro, Phys. Rev. B **61**, R7831 (2000). Note that one dimensionality is better evidenced by optical measurements than by dc conductivity measurements [see the case of the blue bronze in G. Travaglini, P. Vachter, J. Marcus, and C. Schlenker, Solid State Commun. **37**, 599 (1981)].

[6] M. Ghedira, M. Anne, J. Chenevas, M. Marezio, and F. Sayetat, J. Phys. C **19**, 6489 (1986).

[7] T. Inami, K. Ohwada, H. Kimura, M. Watanabe, Y. Noda, H. Nakamura, T. Yamasaki, M. Shiga, N. Ikeda, and Y. Murakami, Phys. Rev. B **66**, 073108 (2002).

[8] O. Massenet, J. J. Since, J. Mercier, M. Avignon, R. Buder, V. D. Nguyen, and J. Kleber, J. Phys. Chem. Solids **40**, 573 (1979).

[9] M. Takano, H. Kosugi, N. Nakanishi, M. Shimada, T. Wada, and M. Koizumi, J. Phys. Soc. Jpn. **43**, 1101 (1977).

[10] L. Forro, R. Gaal, H. Berger, P. Fazekas, K. Penc, I. Kezsmarki, and G. Mihaly, Phys. Rev. Lett. **85**, 1938 (2000).

[11] T. Graf, D. Mandrus, J. M. Lawrence, J. D. Thompson, P. C. Canfield, S. W. Cheong, and L. W. Rupp, Phys. Rev. B **51**, 2037 (1995).

[12] H. Imai, H. Wada, and M. Shiga, J. Phys. Soc. Jpn. **65**, 3460 (1996).

[13] H. Nakamura, H. Tanahashi, H. Imai, M. Shiga, K. Kojima, K. Kakurai, and N. Nishi, J. Phys. Chem. Solids **60**, 1137 (1999).

[14] H. Nakamura, H. Imai, and M. Shiga, Phys. Rev. Lett. **79**, 3779 (1997).

[15] H. Nakamura, T. Yamasaki, S. Giri, H. Imai, M. Shiga, K. Kojima, M. Nishi, K. Kakurai, and N. Metoki, J. Phys. Soc. Jpn. **69**, 2763 (2000).

[16] L. F. Mattheiss, Solid State Commun. **93**, 791 (1995).

[17] M. H. Whangbo, H. J. Koo, D. Dai, and A. Villesuzanne, J. Solid State Chem. **165**, 345 (2002); E. Canadell (private communication).

[18] J. P. Pouget, in [19], p. 87.

[19] *Low Dimensional Electronic Properties of Molybdenum Bronzes and Oxides*, edited by C. Schlenker (Kluwer, Dordrecht, 1989).

[20] The Curie constant is $C = np_{\mathrm{eff}}^2\mu_B^2$, where n is the spin density and p_{eff} the effective Bohr magneton, equal to 1.73 for V^{4+}. One $s = 1/2$ spin every other V site ($n = 0.5$) yields an effective moment divided by $\sqrt{2}$, i.e., $1.223\mu_B$.

[21] E. Sandré, P. Foury-Leylekian, S. Ravy, and J.-P. Pouget, Phys. Rev. Lett. **86**, 5100 (2001).